KINETICS OF TEMPERATURE-PROGRAMMED REACTIVATION OF A HYDRODESULPHURIZATION CATALYST

Pavel Fott[a] and Pavel Šebesta[b]

[a] *Institute of Chemical Process Fundamentals, Czechoslovak Academy of Sciences, 165 02 Prague 6*, and*
[b] *Institute of Geology and Geotechnics, Czechoslovak Academy of Sciences, 182 09 Prague 8*

Received December 22nd, 1982

The kinetic parameters of reactivation of a carbonized hydrodesulphurization (HDS) catalyst by air were evaluated from combined thermogravimetric (TG) and differential thermal analysis (DTA) data. In addition, the gaseous products leaving a temperature-programmed reactor with a thin layer of catalyst were analyzed chromatographically. Two exothermic processes were found to take part in the reactivation, and their kinetics were described by 1st order equations. In the first process (180–400 °C), sulphur in Co and Mo sulphides is oxidized to sulphur dioxide; in the second process (300–540°C), in which the essential portion of heat is produced, the deposited carbon is oxidized to give predominantly carbon dioxide. If the reaction heat is not removed efficiently enough, ignition of the catalyst takes place, which is associated with a transition to the diffusion region. The application of the obtained kinetic parameters to modelling a temperature-programmed reactivation is illustrated on the case of a single particle.

The principal cause of the decrease in the activity of catalysts during the catalytic process is deposition of carbon (coke) on their surface. The activity can be restored to nearly its initial value by reactivation consisting in a removal of the deposits by controlled oxidation.

At lower temperatures, where the combustion of the deposits is not very vigorous, the mass transport and heat transfer are sufficient to eliminate concentration and temperature differences between the centre of the catalyst particle and the streaming gas, and the reaction proceeds in the kinetic region. As follows from the extensive kinetic study of reactivation of carbonized catalysts (*e.g.*, refs[1–3]; for a survey see ref.[4]), the reaction of carbon with oxygen is first order with respect to the two reacting components; only if the mass concentration of carbon is higher than as corresponds to its monolayer (approximately 5% per 100 m^2/g surface area), the reaction order with respect to carbon is lower at the beginning of the reaction. The rate of reactivation is comparable with that of oxidation of graphite unless transition metals are present in the catalyst; otherwise the reaction proceeds appreciably faster.

At high temperatures the reaction is so fast that the mass transport fails to make up for the concentration differences; a sharp boundary is established between the unreacted shrinking core and the reacted inert layer. The rate of the reaction taking place at this interface is determined by the rate of oxygen diffusion through the reacted inert layer. The kinetics of reactivation in this diffusion region has been treated[2,5] in terms of this concept.

* For the present address see[b].

In the intermediate region between these cases, smooth concentration profiles of both the gaseous and the solid components are established within the particle. The mathematical treatment of the reaction in this region is rather complicated; suitable procedures for the solution of an isothermal particle were only published in the late seventies[6]. The stability analysis[7], however, indicates that for highly exothermic oxidations the reaction course in this intermediate region is unstable, a rapid transition to the diffusion region taking place after the ignition temperature is surpassed. In this region, where the reaction proceeds rapidly particularly in the initial stage, the catalyst may overheat to lose its activity irreversibly. The maximum temperature difference between the particle and the gas in the diffusion region can be calculated by the method of Luss and Amundson[8].

The problem of preventing the catalyst from overheating is of practical importance. For the catalyst reactivation directly in the catalytic reactor, the air delivered is usually rarefied appreciably with nitrogen[9] or steam[10] to reduce the reaction rate. If the reactivation is carried out off the catalytic reactor[11,12], the catalyst is formed into a thin layer on a moving conveyer belt (grid); the reactivation is initiated at a low temperature, raised gradually during the reaction. The air flow rate must be held high enough for an efficient removal of the reaction heat and prevention of the catalyst from ignition. Understanding the kinetics of processes taking place during the oxidation of a carbonized catalyst is prerequisite for designing a suitable reactivation equipment and adjusting the appropriate technological conditions.

In the majority of papers concerned with the reactivation of catalysts[1-5], only the combustion of carbon in the deposit has been so far dealt with. However, with hydrodesulphurization (HDS) catalysts the situation is more intricate, sulphides of cobalt and molybdenum being also oxidized to the corresponding oxides. The kinetics of the processes involved has not been as yet describe.

The aim of the present study was to identify the reactions participating in the oxidation reactivation of a cobalt–molybdenum HDS catalyst and to determine their kinetic parameters. A combination of thermogravimetry (TG) and differential thermal analysis (DTA) was employed for this purpose. For the identification of the processes, the combustion products formed in a temperature-programmed reactor (TPR) were also analyzed. This approach was applied with a view to using the results for modelling the course of the reactivation in a thin catalyst layer where the temperature of the admitted air is gradually increased.

THEORETICAL

In the study of the reaction kinetics in solid–gas systems, data are usually treated in the form of the dependence of mass or concentration on time, measured in isothermal differential reactors for several temperature levels. Methods have also been devised based on nonisothermal data obtained with a linearly increasing temperature[13-15], where the quantities followed are the temperature dependences of the mass loss (TG), or of the temperature difference between sample and environment, or of the concentration of the gaseous component. Here the following conditions must be satisfied: the temperature difference between sample and the surrounding gas must be low enough to ensure a linear sample temperature rise with time; the gas flow through the cell must be fast enough for the conditions to approach those in a differential reactor;

the grains of the solid should be small in size for the reaction to proceed in the kinetic region; and the sample should be in a good contact with the streaming gas.

The used nonisothermal method appears adequate for the description of the reactivation kinetics of HDS catalysts at a programmed temperature rise. The integrated form of the kinetic equation was used for the evaluation of the kinetic parameters; this approach seems to be the most suitable with regard to the nature of TG data. Since the reactivation is 1st order with respect to the solid as well as to oxygen, the integration of the kinetic equation, in the conditions of a linear temperature rise ($T = T_0 + \theta t$) and a constant partial pressure of oxygen, is a simple matter. We can write

$$-\mathrm{d}Y/dT = (Z/\theta)\exp(-E/RT)\,Y, \tag{1}$$

where $Y = c_s/c_s^0$ and $\theta = \mathrm{d}T/\mathrm{d}t$. The fraction of the unreacted solid (carbon), Y, is calculated as

$$Y = \exp(-I), \tag{2}$$

where

$$I = (Z/\theta)\int_{T_0}^{T}\exp(-E/RT)\,\mathrm{d}T. \tag{3}$$

If the reaction does not yet proceed at temperature T_0, this integral can be expressed as a series[13]

$$I = (ZT/\theta)\exp(-U)\,(1/U - 2/U^2 + 6/U^3 \ldots), \tag{4}$$

where $U = E/RT$.

The kinetic parameters Z and E are determined from the experimental dependence of Y on temperature. If the parameters are determined from the TG measurements, the fraction of the unreacted solid is determined as

$$Y = (w_\infty - w)/(w_\infty - w_0) \tag{5}$$

whereas if DTA data are employed, Y can be calculated as[15]

$$Y = \int_{T}^{T_\infty}\Delta T\,\mathrm{d}T \Big/ \int_{T_0}^{T_\infty}\Delta T\,\mathrm{d}T. \tag{6}$$

The integral in the denominator of Eq. (6) equals the area enclosed by the DTA peak, the integral in the numerator is the corresponding fraction of this area. The E and Z parameters are determined by minimizing a response function, which is conveniently chosen in the form (nonlinear regression)

$$Q(Z, E) = \sum_i (Y_i^{\mathrm{cal}} - Y_i^{\mathrm{obs}})^2, \tag{7}$$

where the subscripts cal and obs refer to the calculated and observed values, respectively.

EXPERIMENTAL

Catalyst. CHEROX 3600 (Chemické závody, Litvinov), a cobalt-molybdenum catalyst (CoO, MoO_3, Al_2O_3), was used. During its pretreatment, Co and Mo oxides are converted in part or totally to the sulphides, which is accompanied by a lowering of the valency of molybdenum (Mo(VI) → Mo(IV)). The samples employed had lost their activity due to the formation of deposit during their 15 months service in the hydrodesulphurization of crude oil. The catalyst had a shape of cylindrical pellets 7·5 mm in diameter and 6·5 mm high, its colour was black in the deactivated state and grey-blue in the reactivated and fresh state. The deactivated catalyst contained 1·54% Co, 5·06% Mo, 10·2% C, 3·7% S, 1·4% H (mass %, all with respect to undried catalyst). The loss by annealing (3 h in vacuum) was 9·4%. The bulk density was 0·72 g/cm^3, density of pellets (appearent) ϱ_p = 1·25 g/cm^3, specific heat c_p = 0·84 J/gK, specific surface area 120 and 180 m^2/g for the deactivated and reactivated samples, respectively.

TG *and* DTA *measurements.* The thermogravimetry data were obtained on a Derivatograph instrument (MOM, Budapest) recording simultaneously the temperature dependences of the sample mass (TG) and the temperature difference between sample and the surrounding atmosphere (DTA). A monolayer of 0·1 to 0·2 g of the ground catalyst (0·16 to 0·25 mm) was laid on platinum plates forming a five-level cascade to ensure a good contact with the atmosphere. The reference (differential) thermocouple was placed in the same type of holder (without sample). The arrangement is shown in Fig. 1. Air in the desired flow rate (1·5 to 2·5 cm^3/s) was supplied to the upper part of the cell through a ceramic tube, and withdrawn through an opening in the cell bottom. The ceramic support of the sample holder is brought out to the balance beam of the instrument.

Temperature-programmed reactor (TPR). In addition to the TG and DTA measurements, experiments were performed in a tubular flow reactor with a linear programming of the temperature of the air supplied. Since the air was delivered in excess, the oxygen concentration in the reactor was virtually identical with that in air. The contents of CO_2, SO_2, H_2O, and CO in the combustion products were monitored at the exhaust.

The reactor (Fig. 2) was constituted by a stainless steel tube, i.d. 6·8 cm and length 30 cm, provided with a heat isolation of a 3 cm layer of kaolin wadding and an asbestos rope. Air entered the bottom part of the reactor, where it was heated by a resistance heating coiled on a ceramic cylinder. The linear temperature rise was provided by a TR 10 thyristor controller equipped with a GP-1 graphic programmer (Development Workshop of the Czechoslovak Academy of Sciences, Prague); the temperature sensor, a platinum resistance thermometer, was in contact with the heating element.

To eliminate radial temperature gradients, the preheated air was passed through a 3 cm layer of ceramic saddles and an additional layer of inert alumina pellets of the same size as the catalyst This layer accomodated thermocouple T1 indicating the temperature of the air supplied. The catalyst bed was constituted by one or three layers of pellets, accomodated in an asbestos tube 2·5 cm high, i.d. 4 cm, which reduced the heat removal through the walls. In experiments with inert pellets, the temperature differences within the bed never exceeded 10°C. Thermocouple T2 was positioned immediately after the catalyst bed in the layer of inert pellets. The two thermocouples (T1, T2) provided data of the temperature difference between the two sides of the catalyst layer, ΔT, in dependence on the temperature of the air delivered, T.

Analysis of the combustion products. The relative contents of the components in the gas products were determined chromatographically on an SCH instrument (Chemoprojekt, Satalice) equipped with a thermal conductivity detector. Samples were injected in 5 min intervals. Carbon dioxide was determined at 50°C in a column of Porapak Q (80–100 mesh, column length 0·5 m, diameter 2 mm, carrier gas H_2, flow rate 30 ml/min). Water and sulphur dioxide were determined simultaneously at 90°C in the same column as CO_2, carbon monoxide was determined at 90°C in a column of molecular sieve 5A (60–80 mesh, column length 1 m, diameter 2 mm, carrier gas H_2, flow rate 30 ml/min). The peak sequence on Porapak Q was: air, CO_2, H_2O, SO_2; on sieve 5A: O_2, N_2, CO. The component contents were evaluated based on the peak heights.

RESULTS AND DISCUSSION

Qualitative Treatment

A typical TG-DTA record is shown in Fig. 3. The DTA baseline was determined based on repeated measurements on the oxidized (reactivated) catalyst (the thin line in Fig. 3). As the DTA record demonstrates, a slightly endothermic process occurs at low temperatures (up to approximately 180 °C). Above 200 °C, two exothermic processes start to appear, characterized by two partly overlapping DTA peaks with their maxima at 295 and 465°C. The mass loss accompanying the first exothermic process is

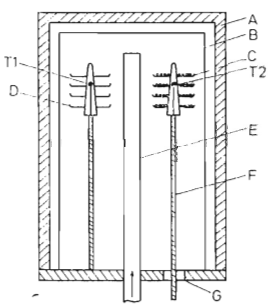

FIG. 1

Cell for TG and DTA measurements. A resistance furnace, B quartz housing, C sample holder D reference holder, E air supply, F support G combustion products withdrawal, T1 reference thermocouple, T2 sample thermocouple

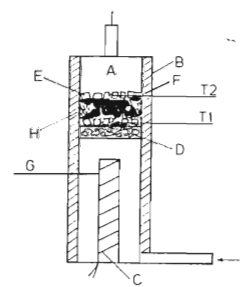

FIG. 2

Temperature-programmed reactor. A reactor, B thermal insulation, C resistance heating, D ceramic saddles, E inert pellets, F catalyst pellets, G platinum thermometer of the controller, H asbestos tube, T1, T2 thermocouples

small, its rate is nearly identical with that of the mass loss after the finished oxidation at temperatures above 540 °C. A marked loss of mass is observed in the temperature region of 300–540°C, the rate of the loss being highest at 460°C.

Experiments in the TPR were carried out using one or three layers of pellets and applying a temperature rise rate of $\theta = 1{\cdot}87$ K/min and a flow rate of $V = 167$ cm^3/s. In the former case, the bed volume was $v = 10$ cm^3, so the space velocity was $V/v = 16{\cdot}7$ s^{-1}; in the latter case, v was 39 cm^3, $V/v = 5{\cdot}56$ s^{-1}. Figs 4 and 5 illustrate experiments in the TPR at the higher space velocity (one pellet layer). The results are presented in the form of dependences of the temperature difference ΔT and the relative contents of CO_2, SO_2, and H_2O on the temperature of the gas supplied. The dependence of ΔT on T (Fig. 4) exhibits two not completely separated peaks with their maxima at about 270 and 410°C. As anticipated, the peak maxima for the TPR are slightly shifted to lower temperatures as compared with the DTA experiments with a faster temperature rise.

As is clear from Fig. 4, the course of the content of SO_2 in the combustion products corresponds with the first peak in the ΔT *vs* T dependence, the content of CO_2 corresponds with the second peak. Water vapour (Fig. 5) is being evolved for nearly the whole time of reactivation (most of it, in the region of 70–200°C). The shape of the dependence of the water content virtually coincides with that obtained for an

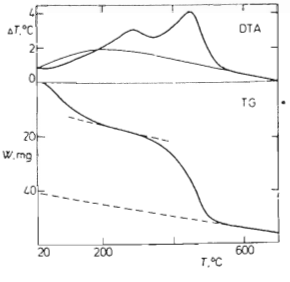

FIG. 3

TG-DTA record. $\theta = 4{\cdot}74$ K/min, $w_0 = 219$ mg; $V = 2{\cdot}5$ cm^3/s; the baseline is drawn in a thin line

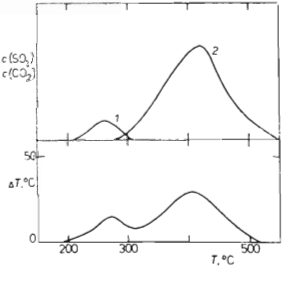

FIG. 4

Dependences of the temperature difference and of the outlet concentrations of SO_2 and CO_2 on the temperature of the air delivered (TPR). Cace without ignition, $\theta = 1{\cdot}87$ K/min, $V/v = 16{\cdot}7$ s^{-1}. *1* SO_2, *2* CO_2

experiment conducted under nitrogen; hence, the majority of the water is desorbed from the catalyst surface rather than formed during the oxidation of the deposit. Water seems to be bonded to the catalyst in several forms whose thermodesorption peaks overlap each other. Because of its low content in the gas, carbon monoxide could not be detected reliably; small amounts were only traced at about 450°C.

The results for the TPR using the lower space velocity (three pellet layers) are summarized in Figs 5 and 6. Below 300°C the ΔT *vs* T plot (Fig. 6) resembles that for the preceding case; at approximately 320°C the dependence rises slowly at the beginning and more rapidly later, and ultimately a dramatic temperature increase appears: the catalyst is ignited (ignition temperature 340°C). After surpassing the temperature of 360°C ($\Delta T = 240$°C), the plot descends rapidly; the catalyst layer becomes extinct at 380°C, and at 400°C, ΔT is as low as 20°C. The dependence ascends again slowly to form a lower peak at 460°C. At 520°C the heat-producing process is virtually finished, the catalyst has been oxidized.

The temperature dependence of the content of CO_2 is similar to that of ΔT starting from the temperature of 300°C. As to SO_2, below 300°C its temperature dependence copies the first peak of the ΔT *vs* T dependence; at 310 – 330°C no SO_2 can be detected, whereas after the ignition it appears again to give rise to a sharp narrow peak, though lower than the corresponding peak of CO_2; and no additional SO_2 is evolved at higher temperatures. Up to the temperature of ignition, the water content varies similarly as in the case without ignition (Fig. 5). The ignition was accompanied by only a twofold increase in the content of water, while the content of CO_2 increased multiply. After the extinction the water content decreased slowly.

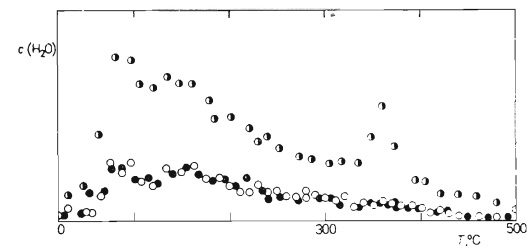

FIG. 5

Dependence of the concentration of water vapour on the temperature of the air delivered (TPR). $\theta = 1{\cdot}87$ K/min; ○ no ignition ($V/v = 16{\cdot}7\ s^{-1}$), ● experiment under nitrogen ($V/v = 16{\cdot}7\ s^{-1}$), ◑ case with ignition ($V/v = 5{\cdot}56\ s^{-1}$)

The results can be interpreted as follows. The initial slightly endothermic process may be associated with the desorption of water. During the first exothermic process, SO_2 is formed by oxidation of sulphides of cobalt and molybdenum to the oxides, *e.g.*, $MoS_2 + \frac{7}{2}O_2 = MoO_3 + 2\,SO_2$. The stoichiometry together with the initial sulphur content (3·7%) accounts for the small mass loss observed during the first process. It is difficult to determine the time that the process is finished because, in view of the lower sensitivity of the analytical method with respect to SO_2, the ending of its peak does not indicate termination of the process. On the contrary, at the moment of ignition the reaction apparently has not finished, SO_2 being detected again as a sharp narrow peak. The termination of the process cannot be determined based on the ΔT record either because the ΔT peaks of the two exothermic processes are not well resolved. The combustion to SO_2 occurred in both cases (slowly) in the kinetic regime, where the rate of the process is determined by the chemical reaction.

In the second exothermic process, which is accompanied by a marked mass loss and generation of a considerable amount of heat, the carbon deposited (10·2%) is burnt to give predominantly carbon dioxide. If the heat is removed efficinetly and the temperature rise is not too rapid, the reaction proceeds slowly near the kinetic region, but if the heat removal is insufficient, the combustion of carbon can bring about unwanted ignition of catalyst. The reaction temperature then increases to the point that diffusion becomes the rate determining step, and the combustion of the deposit can be treated in terms of the shrinking unreacted-core model in which the

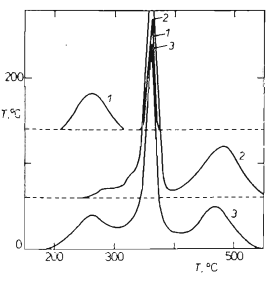

FIG. 6

Dependences of the temperature difference and of the outlet concentrations on the temperature of the air delivered (TPR). $\theta = 1{\cdot}87$ K/min, $V/v = 5{\cdot}56\ s^{-1}$ (ignition); *1* SO_2, *2* CO_2, *3* ΔT

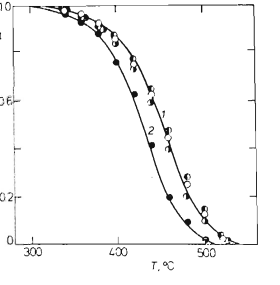

FIG. 7

Kinetics of the second exothermic process. Experimental values from the TG measurements (Table I); series: ○ 1, ◐ 2, ◑ 3, ● 4. The curves correspond to calculated dependences, θ (K/min): *1* 4·6, *2* 2·15

process is controled by the diffusion through the reacted inert layer. Immediately after the ignition the reacted layer is very thin and thus the rate of combustion and consequently also the catalyst temperature are highest[8]. As the thickness of the reacted layer increases, the reaction rate decreases since the diffusion path length is extended and the interface area reduced. As a consequence, the rate of heat generation also diminishes and the reaction becomes extinct.

The shrinking unreacted core could be observed on sections of the pellets taken out in various time intervals after the catalyst ignition; the unreacted core was dark in colour, whereas the oxidized layer was light grey-blue. Pellets taken out of the reactor immediately before the ignition were uniformly dark across the entire cross section; this bears out the assumption that before the ignition the reaction occurs in the kinetic region across the pellet bulk. Unless ignition took place, the colour of the section varied with increasing temperature from dark black through grey to light grey-blue; the colour was uniform across the section, hence, the reaction occurred in the kinetic region. Similar differences in the pellet sections for the kinetic and the diffusion regimes have been observed by Weisz and Goodwin[5].

Since up to the moment of ignition the reaction occurs near the kinetic region, the kinetics of the chemical processes determining the reactivation rate are relevant for the kinetic description of the temperature-programmed reactivation.

Kinetic Parameters

The kinetic parameters of the reactivation were evaluated based on four thermogravimetric measurements whose conditions are given in Table I. The partial pressure of oxygen in the sample cell was deemed constant and equal to that in air. As follows from a mass balance of the cell, for the maximum observed rate of oxidation of

TABLE I

Conditions of the TG and DTA measurements. Grain size 0·16—0·25 mm

Series No	θ K/min	W_0 mg	V cm^3/s	Technique[a]
1	4·46	127	1·67	TG
2	4·55	104	2·5	TG
3	4·74	219	2·5	TG + DTA
4	2·15	139	2·5	TG

[a] Technique used for the evaluation of the kinetics.

6 μmol/g s and the lowest applied value of $V/w_0 = 11{\cdot}4$ cm^3/g the partial pressures of oxygen in the cell and in air should not differ more than by 6%.

The kinetic parameters Z_{II} and E_{II} of the second exothermic process were evaluated from all of the TG records. The Y values were read in ten-degree intervals in the region of 300 – 540°C. As can be seen in Fig. 3, the mass loss curve decreases slowly linearly also after surpassing the temperature of 540°C, and virtually the same decrease is observed also at temperatures below 300°C. Therefore, the mass values used for the calculation of Y according to Eq. (5) were taken with resecpt to the baseline obtained by extending the straight line from the range of 540 – 700°C. The points of the dependence of Y_{II} *vs* T so obtained for all the four measurement series are plotted in Fig. 7. The reproducibility of measurement is good, the dependences for series 1 – 3, with a virtually identical temperature rise rate of $\theta = 4{\cdot}6$ K/min, approach each other closely although the weight of the samples was different. For $\theta = 2{\cdot}15$ K/min the curve is somewhat shifted to lower temperatures, as anticipated.

The Z_{II}, E_{II} parameters were calculated by nonlinear regression from the whole data set, and for a comparison, also from the individual series. Marquardt's method was applied to the minimization of the response function Q (Eq. (7)). The results of the regression analysis are summarized in Table II. The activation energy is determined reliably, its values for the various series approaching each other closely. The resulting activation energy of the HDS catalyst, 110·4 kJ/mol, compares well with the data of Hano and coworkers[3] for a transition metals-containing catalyst (catalyzed combustion of carbon), but is lower than the value reported for an alumosilicate catalyst free of transition metals[1]. For the frequency factor (Table II) the differences between the various series are appreciably higher, which can be explained in terms of the high correlation between the Arrhenius equation parameters reported in literature[16].

TABLE II
Kinetic parameters of the second exothermic process

Series No	Z_{II} 10^3 s^{-1}	E_{II} kJ/mol	s^a
1	107·2	109·6	0·011
2	52·8	105·9	0·019
3	38·9	103·4	0·012
4	138·5	111·7	0·015
1 + 2 + 3 + 4	122·5	110·4	0·028

[a] Standard deviation.

A reliable result is thus not a single Z, E pair corresponding to the minimum of the response function $Q(Z, E)$, but rather a region of Z, E pairs (confidence interval) for which the response function (sum of squares of deviations) lies below its critical value. This critical value can be determined, for a preselected level of probability (95%), by Beale's criterion[17]. For the Arrhenius equation the range of possible Z, E is very narrow[16]; it turned out that in log Z, E coordinates it can be approximated by a line segment (Fig. 8). All of the Z, E pairs calculated for the various series are found within the confidence interval established for the whole set. Thus high-quality kinetic results can be expected to obtain even from a single thermogravimetric measurement. Fig. 7 shows the kinetic plots for the parameters obtained from the whole set (series 1–4); the calculation agrees well with the experiment for the two temperature rise rates applied.

The Z_I, E_I parameters for the first exothermic process could not be calculated from the TG record since no appreciable mass loss appeared. For an evaluation from the DTA data, record No 3 was employed (Table I, Fig. 3) obtained with a double sample weight. Fig. 9 presents the temperature dependence of the temperature difference, derived from the DTA record with baseline correction. The parameters cannot be evaluated directly from the DTA peak according to Eq. (6) because the peak overlaps partly with that of the second exothermic process.

The method used for the determination of the parameters E_I, Z_I is based on combined TG-DTA data, assuming that the two processes, I and II, are mutually inde-

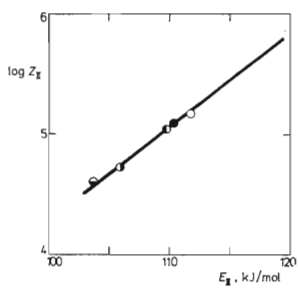

FIG. 8

Confidence interval of the Z_{II}, E_{II} parameters. The parameter pairs were calculated from the sets (Table II): ◐ 1, ◑ 2, ◒ 3, ○ 4, ● 1 + 2 + 3 + 4

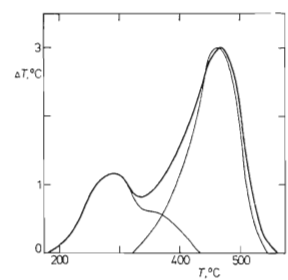

FIG. 9

Dependence of the temperature difference on temperature (DTA). $\theta = 4{\cdot}74$ K/min. The thin lines indicate peaks corresponding to the exothermic processes I and II

pendent and can be described by 1st order equations,

$$-\mathrm{d}Y_i/\mathrm{d}T = (Z_i/\theta)\exp(-E_i/RT)\,Y_i\,, \quad i = \mathrm{I}, \mathrm{II}\,. \tag{8}$$

The character of the TG and DTA data of a carbonized catalyst is taken into account: process II can be evaluated from the TG record, and its reaction heat and concentration of the reacting component are known ($C + O_2 = CO_2$, ΔH (350°C) = −383·8 kJ/mol; c_s^0 = 0·00833 mol/g); process I is accompanied by no appreciable mass loss, its reaction heat and concentration of the reacting component are unknown, but there is a definite heat effect involved and its DTA peak is separated, in part at least, from that of process II.

The parameters of the first process were determined as follows:

1) The Z_{II}, E_{II} parameters were determined from the TG record; E_{II} = 110·4 kJ/mol, Z_{II} = 122 500 s^{-1}.

2) The area A_{II} beneath the second DTA peak was determined; this area is proportional to the heat evolved in the second process,

$$A_{II} = \int_{(T_0)_{II}}^{(T_\infty)_{II}} \Delta T_{II}\,\mathrm{d}T\,. \tag{9}$$

By combining Eqs (*6*), (*8*), (*9*),

$$A_{II} = \theta\,\Delta T_{II}/[Z_{II}\exp(-E/RT)\,Y_{II}]\,. \tag{10}$$

For the calculation of A_{II} according to Eq. (*10*), any T, ΔT_{II} pair can be used in the temperature region where process I is finished, hence, where $\Delta T = \Delta T_{II}$. Actually, the pair corresponding to the maximum of the second DTA peak was taken: T = = 465°C, ΔT = 3°C. The Y_{II} value was calculated from Eq. (*2*). In this manner, A_{II} was established to be 325 K^2.

3) Eq. (*10*) was treated using the obtained Z_{II}, E_{II}, A_{II} constants and the calculated dependence of Y_{II} on T to calculate the separate DTA peak of the second exothermic process, hence the ΔT_{II} *vs* T dependence.

4) The separate peak of the first process ($\Delta T_I = \Delta T - \Delta T_{II}$) was obtained as the difference between the experimental dependence ΔT *vs* T and the calculated dependence ΔT_{II} *vs* T. The separate peaks are drawn in a thin line in Fig. 9.

5) The area beneath the DTA peak for process I was obtained by numerical integration (Eq. (*6*)), A_I = 154 K^2; the dependence of Y_I *vs* T was also evaluated using Eq. (*6*) (Fig. 10).

6) The kinetic parameters of the first process, Z_I, E_I, was determined from the de-

pendence of Y_I *vs* T similarly as for the second process; the results are given in Table III. The fit of the calculated dependence to the observed Y values (Fig. 10), in terms of the standard deviation from the regression curve, is somewhat poorer for the first process ($s = 0{\cdot}037$) than for the second one (Table II), evaluated from more precise TG data.

7) The heats produced by the two processes per unit mass of catalyst, q_I and q_{II}, were calculated as $q_{II} = -\Delta H_{II}(c_S^0)_{II}$, $q_I = (A_I/A_{II})\, q_{II}$ (Table III).

In this manner, all the parameters were calculated in the equation for the rate of heat generation in the reactivation,

$$\sum_{i=I,II} -\mathrm{d}c_{si}(-\Delta H_i)/\mathrm{d}t = \sum_{i=I,II} -q_i\, \mathrm{d}Y_i/\mathrm{d}t\,, \qquad (11)$$

where

$$-\mathrm{d}Y_i/\mathrm{d}t = Z_i \exp\left(-E_i/RT(t)\right) Y_i\,, \quad i = I, II\,; \qquad (12)$$

$T(t)$ is an arbitrary dependence of catalyst temperature on time.

TABLE III

Kinetic parameters of reactivation

Process	E kJ/mol	Z s^{-1}	q kJ/g
I	48·4	25·6	1·55
II	110·4	122 500	3·28

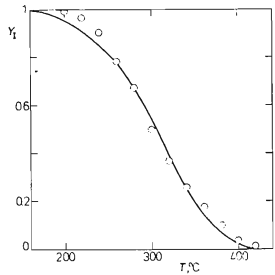

FIG. 10

Kinetics of the first exothermic process. The experimental data were derived from combined TG and DTA measurements; $\theta = 4{\cdot}74$ K/min. The curve corresponds to the calculated dependence

An Example of Modelling a Temperature-Programmed Reactivation

Eqs (*11*), (*12*) with parameters of Table III can be employed for a modelling of the behaviour of a particle or a reactor in the temperature-programmed reactivation with air. For an illustration, we shall treat the simplest case of a single particle. Assuming that (till the moment of ignition) the reactivation occurs in the kinetic region and the resistance to heat transfer is concentrated in a film surrounding the particle[8], the heat balance in a temperature-programmed reactivation of the particle, *i.e.* at a linearly increasing temperature of the air suppiled, can be written as

$$\mathrm{d}\,\Delta T/\mathrm{d}T = \sum_{i=\mathrm{I,II}} Z_i \exp\left[-E_i/R(T+\Delta T)\right] Y_i q_i/(\theta c_p) - 3h\,\Delta T/(a\varrho_p \theta c_p)\,. \qquad (13)$$

At the same time,

$$\mathrm{d}Y_i/\mathrm{d}T = -(Z_i/\theta)\exp\left[-E_i/R(T+\Delta T)\right] Y_i\,, \quad i = \mathrm{I, II}\,. \qquad (14)$$

The initial conditions for this system of differential equations are

$$T = T_0\,, \quad \Delta T = 0\,, \quad Y_\mathrm{I} = 1\,, \quad Y_\mathrm{II} = 1\,. \qquad (15)$$

Here ΔT is the temperature difference between the particle and the air. The following constants were adopted: $\varrho_p = 1{\cdot}25$ g/cm^3, $c_p = 0{\cdot}84$ J/gK, $a = 0{\cdot}36$ cm.

As will be clear from Eqs (*13*)–(*15*), the temperature dependences of ΔT, Y_I, and Y_II will only depend on the temperature increase rate θ and on the heat transfer coefficient which in turn depends on the linear velocity of gas[18]. Numerical solution of the system (*13*)–(*15*) (by the Runge–Kutta method with an automatic step control)

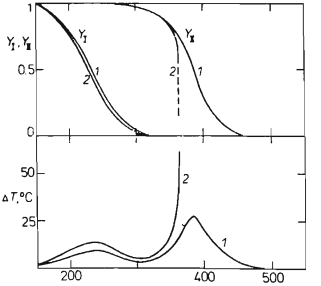

FIG. 11

Modelling the behaviour of a catalyst particle during the temperature-programmed reactivation. $\theta = 0{\cdot}95$ K/min, h (J/cm^2 s K): *1* $4{\cdot}25 \cdot 10^{-3}$, *2* $2{\cdot}87 \cdot 10^{-3}$

revealed that at low θ or high h values the particle is reactivated slowly in the kinetic region (Fig. 11, case 1), whereas at higher θ or lower h values the ΔT *vs* T plot starts suddenly to bend upwards and the Y_{II} *vs* T plot downwards (Fig. 11, case 2): the catalyst is ignited, the heat evolved is not removed efficiently enough, and a transition to the diffusion region takes place. Our simplified model fails to account for the behaviour of a particle in the diffusion region; the method of Luss and Amundson[8], requiring the knowledge of the effective diffusivity, should be applied to this case.

LIST OF SYMBOLS

A	area enclosed by the DTA peak
a	particle diameter
c_s, c_s^0	concentration of the solid component and its initial value; $c_s = n_s/w_0$
c_p	specific heat of catalyst
E	activation energy
h	heat transfer coefficient
ΔH	heat of reaction
i	subscript (i = I, II)
I	integral, Eq. (*3*)
n_s	amount of substance of the solid component (mol)
Q	response function, Eq. (*7*)
q	heat of reaction with respect to the initial amount of catalyst
R	gas constant
t	time
T, T_0. T_∞	temperature, initial temperature, final temperature
ΔT	temperature difference
U	variable, $U = E/RT$
V	air flow rate before entering the reactor or cell
v	catalyst bed volume
w, w_0, w_∞	catalyst mass: at temperature T, initial, and after the reaction
Y	fraction of the unreacted solid component
Z	frequency factor
θ	temperature rise rate; $\theta = \mathrm{d}T/\mathrm{d}t$
ϱ_p	apparent initial density of catalyst

REFERENCES

1. Weisz P. B., Goodwin R. D.: J. Catal. *6*, 227 (1966).
2. Mickley H. S., Nestor J. W., Gold L. A.: Can. J. Chem. Eng. *43*, 61 (1965).
3. Nano T., Nakashio F., Kusunoki J.: J. Chem. Eng. Jap. *8*, 127 (1975).
4. Satterfield Ch. N.: *Mass Transfer in Heterogeneous Catalysis*. MIT Press, Cambridge 1970.
5. Weisz P. B., Goodwin R. D.: J. Catal. *2*, 397 (1963).
6. Boersma M. A. M., Spierts J. A. M., Van der Baan H. S.: Chem. Eng. Sci. *35*, 1237 (1980).
7. Ishida M., Wen C. Y., Shirai T.: Chem. Eng. Sci. *29*, 1043 (1971).
8. Luss D., Amundson N. R.: AICHE J. *15*, 194 (1969).
9. Byrns A. C., Bradley W. E., Lee M. W.: Ind. Eng. Chem. *35*, 1160 (1943).
10. Cole R. M., Davidson D. D.: Ind. Eng. Chem. *41*, 2711 (1949).

11. Kunzelman R. C., Mantis J. H.: Ann. Inst. Belge Pétrole *14* (2), 33 (1980).
12. Kruk A. V. D.: Pétrole at techniques *277*, 49 (1981).
13. Šesták J.: Silikáty *11*, 153 (1967).
14. Wendlandt W. W.: *Thermal Methods of Analysis*. Wiley, New York 1974.
15. Škvára F., Šatava V.: J. Therm. Anal. *2*, 325 (1970).
16. Kittrel J. R.: Advan. Chem. Eng. *8*, 98 (1970).
17. Beale E. M. L.: J. Roy. Stat. Soc. B *22*, 41 (1960).
18. Szekely J., Evans J. W., Sohn H. Y.: *Gas–Solid Reactions*. Academic Press, New York 1976.

Translated by P. Adámek.